ADVANCED MATERIALS INTERFACES
www.advmatinterfaces.de

Kinetics of Photoinduced Wettability Switching on Nanoporous Titania Surfaces under Oil

Divya Panchanathan, Gibum Kwon, Talal F. Qahtan, Mohammad A. Gondal, Kripa K. Varanasi, and Gareth H. McKinley**

Titanium dioxide (titania or TiO_2) is well known for its photocatalytic properties and its ability to remove organic contaminants under UV light illumination. It is also known to switch its surface wetting characteristics from being hydrophilic to superhydrophilic under exposure to UV light in air. However, less is known about the switching of the hydrophilicity of TiO_2 surfaces immersed in an oil medium. In this work, self-assembled TiO_2 nanoparticle surfaces are immersed in an oil environment, and the kinetics of contamination-induced hydrophobicity and photoinduced hydrophilicity are studied using in situ contact angle measurements. A simple model is developed to relate the evolution in the measured contact angle to photocatalytically induced changes on the surface of nanoporous titania by integrating the Langmuir–Hinshelwood adsorption isotherm with the Cassie–Baxter analysis of the effective contact angle of a drop sitting on a composite surface. The resulting model can be used to predict and control wetting kinetics in drop coalescence applications. Moreover, it is shown that immersed oil–water separation membranes which have been fouled by low surface tension contaminants can be rapidly recovered in situ using this underwater photocatalytic reaction without the need for backwashing or harsh chemical reagents.

1. Introduction

Photo-responsive titanium dioxide (TiO_2) surfaces, which exhibit switching in their surface wettability states from hydrophilic (i.e., with contact angle for water ("w"), $\theta_w \leq 90°$)[1,2] to superhydrophilic (i.e., $\theta_w \leq 5°$)[1,3] under UV illumination,[4–6] have been widely utilized in a broad range of surface engineering applications including self-cleaning,[7,8] antifogging,[6,9] and oil–water separation.[9,10]

A large number of studies have focused on understanding the origin of this pronounced wettability switch of TiO_2 surfaces.[4,7] Among various proposed mechanisms, two distinct schools of thoughts have been promulgated to explain the large changes in photoinduced wettability of TiO_2 surfaces. The first viewpoint argues that photocatalytic oxidation or reduction of adsorbed organic contaminants leads to increased exposure of the underlying bare TiO_2 surface which is inherently hydrophilic.[11–14] The second is based on the surface reconstruction of TiO_2 resulting in a local increase of hydroxyl species (due to molecular or dissociative adsorption of water molecules) which promote hydrophilicity.[15–18] Although a final unified mechanism is still under debate, the ultimate effect of UV light illumination on TiO_2 surfaces is the evolution of heterogeneity in the local surface chemistry and a progressive increase in surface energy which drives increased wettability by polar liquids such as water.[19–21]

Contact angle measurements with sessile drops have been widely employed as a means of characterizing the surface wettability of chemically heterogeneous or topographically structured surfaces.[22–26] The contact angle for a sessile droplet on a chemically heterogeneous surface can be described by the Cassie–Baxter equation[27,28] given by

$$\cos\theta^* = f_1 \cos\theta_1 + f_2 \cos\theta_2 \quad (1)$$

Here, θ^* is the apparent contact angle of a liquid drop placed on a heterogeneous surface that consists of phase 1 and phase 2. f_1 and f_2 are the area fractions of each phase whereas θ_1 and θ_2 are the Young's contact angles of the same liquid on homogeneous surfaces of phase 1 and phase 2, respectively. The cosine of the measured contact angle (θ^*) on a chemically heterogeneous surface is therefore approximately the area-weighted average of the cosine of the contact angles measured on homogeneous surfaces of phase 1 and phase 2.

Only a few studies have developed kinetic models that characterize the time-dependent evolution in surface chemistry heterogeneity of a photocatalytic surface using contact angles

D. Panchanathan, Prof. K. K. Varanasi, Prof. G. H. McKinley
Department of Mechanical Engineering
Massachusetts Institute of Technology
Cambridge, MA 02139, USA
E-mail: varanasi@mit.edu; gareth@mit.edu
Dr. G. Kwon
Department of Mechanical Engineering
University of Kansas
Lawrence 66045, USA
T. F. Qahtan, Prof. M. A. Gondal
Physics Department
King Fahd University of Petroleum and Minerals
Dharan 34464, Saudi Arabia
The ORCID identification number(s) for the author(s) of this article can be found under https://doi.org/10.1002/admi.201700462.

DOI: 10.1002/admi.201700462

measured under UV light illumination.[19–21,29] One of the earliest quantitative models proposed by Sakai et al. suggested that the reciprocal of the water contact angle increases linearly with increasing UV light illumination time.[29] Later, Seki and Tachiya incorporated the fact that the area fraction of hydrophilic regions increases due to the additional hydroxyl species generated by UV light illumination.[20] They also demonstrated that using the cosine values of measured water contact angles is more appropriate for quantifying the kinetics of the wettability conversion. More recently, Foran et al. have proposed a relationship between the kinetics of photocatalytic destruction of surface adsorbed organic molecules and the contact angles for water droplets on TiO_2 surfaces exposed to UV light illumination in air.[19]

Although these studies have helped to elucidate the kinetics of photoinduced wettability switching of TiO_2 surfaces and provided valuable insights into the mechanism, they typically neglect the presence of dynamic organic contamination on TiO_2 surfaces. Such contamination is unavoidable due to the intrinsic high surface energy of a titania surface.[30,31] Fouling by organic materials (e.g., oil) can be observed in an oil–water separation membrane where the membrane surface is modified with hydrophilic TiO_2.[32] While there are a few reports of photoinduced hydrophilicity switching on TiO_2 surfaces submerged in an oil environment, they do not study the kinetics of the processes involved in detail.[33–36] The aim of the present study is to take into account the kinetics of adsorption, desorption, and photocatalytic breakdown of oily contaminants on titania in order to quantitatively describe the kinetics of photoinduced wettability switching on TiO_2 surfaces that may find future applications in oil–water separation technologies.

In order to study the kinetics of the photoinduced wettability switching of TiO_2 surfaces submerged in an oil environment through the application of goniometry, it is necessary to first understand the relationship between the contact angles of sessile water drops measured on a surface in air and those measured on the same surface submerged under oil. Liu et al.[37] and Jung and Bhushan[38] were among the first to study underwater oleophobicity and relate the underwater contact angles of sessile oil droplets to the in-air contact angles of sessile water and oil drops. By following a similar derivation, we obtain an expression for the contact angle of sessile water drops on a surface immersed in an oil environment

$$\cos\theta_{w,o} = \frac{\gamma_{w,a}\cos\theta_{w,a} - \gamma_{o,a}\cos\theta_{o,a}}{\gamma_{o,w}} \quad (2)$$

where $\theta_{w,a}$, $\theta_{o,a}$, and $\theta_{w,o}$ are, respectively, the contact angles of water drop-in-air, oil drop-in-air, and water drop-in-oil; similarly, $\gamma_{w,a}$, $\gamma_{o,a}$, and $\gamma_{o,w}$ are the respective interfacial tensions between the corresponding phases. From Equation (2), it is evident that an in-air hydrophilic-oleophilic surface (i.e., with $\theta_{w,a} < 90°$, $\theta_{o,a} < 90°$) can display under-oil hydrophilicity ($\theta_{w,o} < 90°$) if the numerator is positive, whereas an in-air hydrophobic-oleophilic surface ($\theta_{w,a} > 90°$, $\theta_{o,a} < 90°$) would display under-oil hydrophobicity ($\theta_{w,o} > 90°$) because the numerator of Equation (2) is always negative.

A clean surface of titania in air is both hydrophilic and oleophilic,[39] and hence is naturally hydrophilic when immersed in oil. However, contamination of a titania surface with a nonfluorinated organic species leads to a lowering of the surface energy and an increase in the water contact angle under oil (because it will become in-air hydrophobic-oleophilic). We have taken advantage of this contrast in water drop-in-oil contact angles between clean and contaminated surfaces to study the dynamics of wettability switching on fully immersed TiO_2 surfaces during contamination and subsequent photocatalytic cleaning.

In this paper, we first describe the layer-by-layer (LBL) self-assembly protocol used to prepare the nanoporous TiO_2 surfaces and quantify the resulting morphology of the surface using profilometry and ellipsometry. We then use time-resolved measurements of effective water contact angles $\theta^*_{w,o}(t)$ for characterizing the surface wettability of the titania surfaces submerged under oil during both contamination and subsequent UV exposure. By combining the Langmuir–Hinshelwood mechanism of photocatalysis and an appropriate Cassie–Baxter description for the effective contact angles of a sessile droplet of water on a textured substrate submerged in an oil environment, we propose a model to directly relate the kinetics of photocatalytic destruction of oil to the change in surface energies (or effective contact angles) for water on immersed titania surfaces under UV light illumination. We estimate the kinetic rate constants of contamination and photocatalysis by fitting our model to the measured changes in the contact angles and explain how these rate constants vary with UV illumination intensity. Finally, we discuss the application of our model to predict drop coalescence and removal of oil from fouled titania surfaces underwater.

2. Results and Discussion

The LBL deposition method[40,41] was utilized to self-assemble coatings of TiO_2 nanoparticles onto two types of substrates—glass slides and stainless steel mesh. Here, 30 bilayers of oppositely charged nanoparticles (TiO_2) and polymer (poly(allylamine hydrochloride)) are electrostatically assembled onto a clean substrate using a dip-coating protocol followed by a calcination step as described in the Experimental Section. The calcination step removes the polymer binder and sinters the particles to form a nanoporous titania film that is free of any organic contaminants. A scanning electron microscopy (SEM) image of the resulting TiO_2 film on a glass slide shows that it is nanoporous and uniform with a thickness ≈120 nm (see **Figure 1**). This was also confirmed using contact profilometry. We also measured the porosity of the film using ellipsometric porosimetry as described by Lee et al.[40] and found it to be 27%.

In order to study the dynamics of contamination of TiO_2 surface by oil, the substrate was submerged in an oil bath for a contamination period (t_c) of $0 < t_c \leq 30$ h at room temperature (≈22 °C). Here, we utilized *n*-dodecane ($\gamma_{o,a} = 25$ mNm^{-1}) as a representative oil that might be encountered in oil/water remediation. Henceforth, the dodecane phase will be referred to simply as oil ("o") in this paper. After the desired time of contamination, the substrates were removed from the oil bath and placed in a quartz cell filled with 20 mL of dodecane to measure the under-oil contact angles for water droplets on the

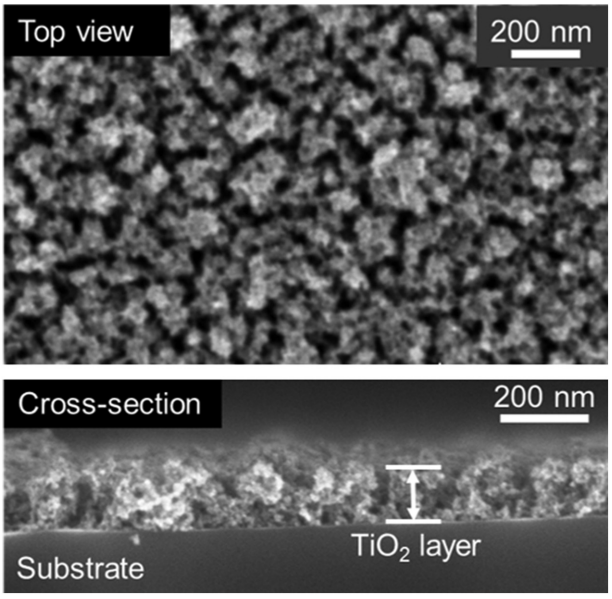

Figure 1. Top and cross-section microscopy image of a layer-by-layer (LBL) self-assembled TiO_2 film (30 bilayers).

contaminated surfaces. A sessile droplet of DI (deionized) water of volume 3 µL was gently placed onto the oil-submerged TiO_2 surface in the quartz cell to measure the apparent contact angle of a water droplet in oil, $\theta^*_{w,o}$, using a contact angle goniometer. The volume of the water droplet was held constant in all contact angle measurements. Note that all of the images obtained from the goniometer have been digitally colored to clearly identify the three phases (blue for water, red for oil, and yellow for solid). UV light was delivered from above the water droplet using a liquid light guide (5 mm spot size) with a visible light filter from a spot UV light curing system as shown in Figure S2 (Supporting Information). The distance between the front face of the UV light optics and the droplet was maintained at 3 mm for all measurements to ensure that the irradiated area was constant. The UV intensity at the surface was varied from 40 to 240 mW cm^{-2} (six intensities, three repetitions each) and this was calibrated ex situ using an UV radiometer.

Since the LBL TiO_2 surfaces possess roughness on nanometric scales, the measured contact angle is the apparent contact angle, θ^* for a liquid droplet sitting on a textured nanoporous titania surface. The as-prepared TiO_2 surface exhibits 0° contact angles for both water ($\theta^*_{w,a}$) and dodecane (oil, $\theta^*_{o,a}$) in an air environment (see **Figure 2**a,b). In-air superomniphilicity (i.e., $\theta^*_{w,a}$ and $\theta^*_{o,a} < 5°$) of the as-prepared TiO_2 surface is due to the combination of intrinsic high solid surface energy of TiO_2 plus the surface roughness that amplifies the wetting behavior of a liquid droplet in the Wenzel state.[3]

When the as-prepared TiO_2 surface was completely submerged in oil, the effective contact angle for a sessile drop of water in oil ($\theta^*_{w,o}$) was measured to be 10° (see Figure 2c). Here, the under-oil water contact angles were measured within a very short period of time (few seconds) after we submerged the surface in an oil bath. Thus, the value reported can be considered to be the contaminant-free (i.e., clean) value for the surface after it is first completely submerged in the oil phase.

However, both the in-air superhydrophilicity and under-oil superhydrophilicity of the as-prepared nanostructured TiO_2 surfaces are altered when the surface is contaminated by adsorbed molecules of oil. Figure 2d–f shows the shape of sessile droplets of oil and water placed on oil-contaminated TiO_2 surfaces. Here, the surfaces are precontaminated by submerging in an oil (dodecane) bath for 18 h. We observe that the contaminated TiO_2 surfaces now exhibit markedly different contact angles $\theta^*_{w,a} = 85^\circ$ and $\theta^*_{o,a} = 0^\circ$, in air (see Figure 2d,e) while the under-oil water contact angle is $\theta^*_{w,o} = 140^\circ$ (see Figure 2f). Thus, it can be seen that, as predicted by Equation (2), the under-oil water contact angle, $\theta^*_{w,o}$ increases drastically as the surface becomes increasingly hydrophobic when contaminated with adsorbed organic molecules. It has been widely reported that organic-contaminated TiO_2 surfaces display markedly higher contact angles with water due to the decreased solid surface energy.[42,43] Consequently, this wettability switch of TiO_2 surfaces (from initial superhydrophilicity to moderate hydrophilicity in-air, and to hydrophobicity under-oil), following prolonged exposure to a low surface energy contaminant such as oil, can be attributed to the increase in the surface area covered by oil. Because the adsorption of organic molecules is a dynamic process,[44,45] we expect that the contact angles measured with sessile water droplets on TiO_2 surfaces will increase with increasing time of adsorption.

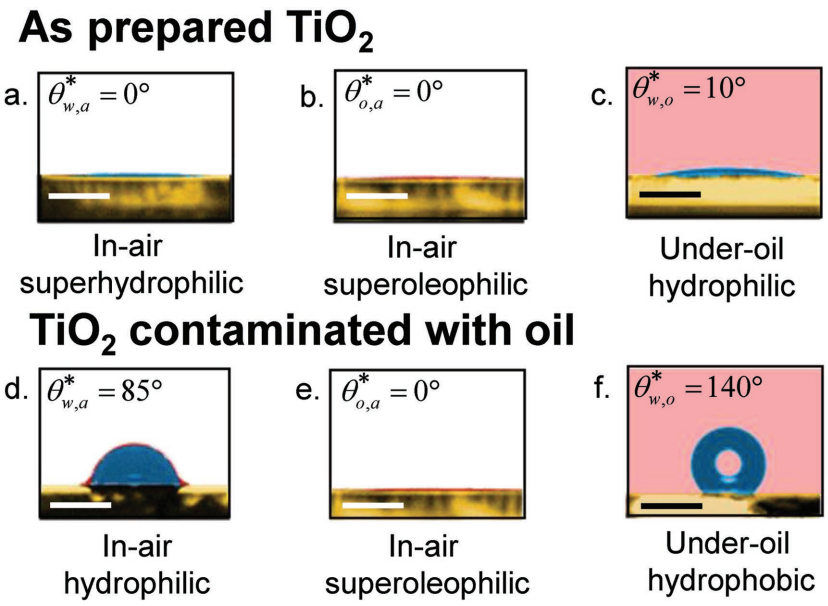

Figure 2. a–c) Contact angles of a sessile water droplet (blue) in air, an oil droplet (red) in air, and a water droplet under-oil on a clean (t_c = 0 min) LBL TiO_2-coated film; d–f) Contact angles of a sessile water droplet in air, an oil droplet in air, and a water droplet under-oil on a fouled (t_c = 18 h) LBL TiO_2-coated film. The scale bar is 1 mm.

In order to study the time-dependent evolution in the surface energy of contaminated TiO_2 surfaces, we conducted under-oil water contact angle ($\theta^*_{w,o}$) measurements on TiO_2 surfaces for a range of times of contamination. In **Figure 3**a, we show the evolution of $\theta^*_{w,o}$ as a function of contamination time (t_c) ranging from 0 to 30 h. The nanotextured TiO_2 surfaces exhibit a gradual increase in $\theta^*_{w,o}$ with increasing time of contamination. The surface was found to transition to a hydrophobic state under oil ($\theta^*_{w,o} > 90^\circ$) when $t_c \approx 10$ h and finally reach complete repellency ($\theta^*_{w,o} \approx 180^\circ$) after $t_c > 27$ h. At this point, a droplet of water placed on the surface immersed in oil can freely roll off the surface. This is consistent with a mechanism in which the entire surface area of the nanostructured titania is slowly covered (contaminated) by a monolayer of adsorbed oil species and reaches saturation at $t_c = 27$ h.

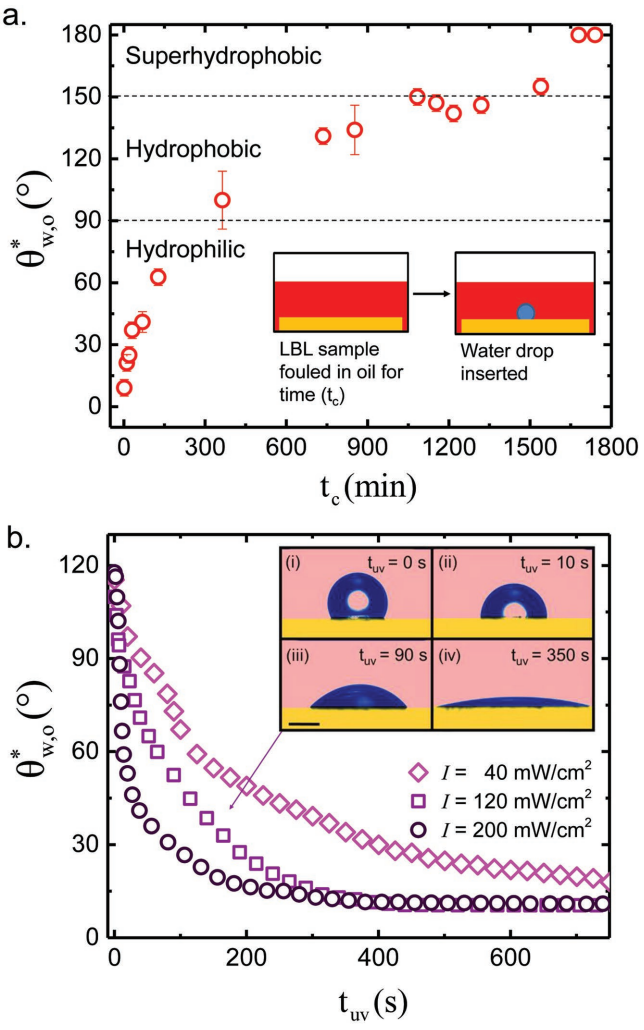

Figure 3. a) Contact angles of a sessile water droplet ($V = 3$ µL) under an oil environment on a LBL TiO_2 surface (30 bilayers) after various time intervals of immersion under oil for contamination. The inset shows the procedure for contamination and subsequent contact angle goniometry using sessile droplets; b) Time-resolved changes in under-oil water contact angles on precontaminated ($t_c = 18$ h) TiO_2 surfaces upon UV light illumination. Here three different UV light intensities are shown ($I = 40$, 120, and 200 mW cm^{-2}). The inset shows a drop of water spreading on a nanostructured TiO_2 surface immersed in dodecane under UV irradiation at $I = 120$ mW cm^{-2} (scale bar = 1 mm).

Under-oil hydrophobic ($\theta^*_{w,o} > 90^\circ$), or superhydrophobic ($\theta^*_{w,o} \geq 150^\circ$) TiO_2 surfaces can reverse their wettability to regenerate their intrinsic superhydrophilic state upon UV light illumination.[33,42] This reversion process is characterized by the decrease in $\theta^*_{w,o}$ upon exposure to UV illumination. We conducted in situ contact angle measurements for sessile water droplets on the precontaminated ($t_c = 18$ h) LBL-assembled TiO_2 surfaces submerged in oil while illuminating them with UV light. In Figure 3b, we show a plot of $\theta^*_{w,o}$ as a function of UV light illumination time (t_{uv}) for three different intensities ($I = 40$, 120, and 200 mW cm^{-2}) on the precontaminated nanostructured TiO_2 surfaces. Before UV light illumination, the precontaminated TiO_2 surface is hydrophobic, displaying $\theta^*_{w,o} = 120^\circ$ (inset (i) in Figure 3b). After the onset of illumination, a droplet of water starts to spread on the surface (insets (ii) and (iii) in Figure 3b), and eventually the surface reverts back to its original under-oil superhydrophilic state characterized by $\theta^*_{w,o} < 10^\circ$ (inset (iv) in Figure 3b). Movie S1 (Supporting Information) demonstrates the UV light-induced spreading of a droplet of water on a precontaminated TiO_2 surface submerged in oil. We also found that the intensity of the UV illumination affects the dynamics of the wettability switching measured on precontaminated TiO_2 surfaces. The rate of initial contact angle decrease becomes larger with increasing illumination intensity. For example, reversion to a superhydrophilic state was completed in a time of $t_{uv} \approx 200$ s, for UV intensity $I = 200$ mW cm^{-2} whereas with a lower intensity of UV light $I = 40$ mW cm^{-2}, a longer illumination time ($t_{uv} > 700$ s) was required to achieve the same superhydrophilic conversion.

The decrease in $\theta^*_{w,o}$ on the contaminated TiO_2 surfaces upon UV light illumination is primarily due to the decrease in the fraction of the surface area covered by adsorbed oil.[19] We attribute this photoinduced cleaning property of TiO_2 surfaces to the photocatalytic destruction of surface-adsorbed hydrocarbon molecules.

The Langmuir–Hinshelwood kinetic model has previously been utilized for characterizing photocatalytic destruction of organic species adsorbed on TiO_2 surfaces.[19,46–48] This model assumes that the surface has a fixed number of sites, each of which can be either occupied by adsorbed organic molecules (i.e., contaminated) or be free of any organic species (i.e., clean). The surface is thus chemically heterogeneous.[49] This kinetic model provides a relation between the overall average surface chemical composition and the rate of photocatalysis of adsorbed organic molecules (as indicated schematically in **Figure 4**). Although the well-known Cassie–Baxter relation can be used to interconnect this chemical heterogeneity of the surfaces to the surface energies of the two states and thus the effective contact angles for sessile liquid drops (see Figure 4), there has been a paucity of quantitative work describing the effect of photocatalysis on the evolution of contact angles in environments where contamination is dynamically occurring. Below we outline the development of a kinetic model that connects the photocatalytic destruction of adsorbed oil under UV light illumination and the evolution in the effective contact angles measured for sessile droplets of water on TiO_2 surfaces submerged in oil.

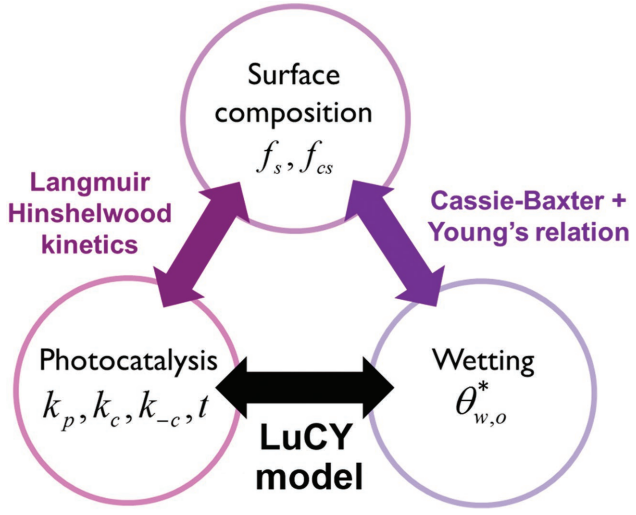

Figure 4. LuCY (Langmuir–Hinshelwood Cassie–Baxter Young) model relates photocatalysis directly to wetting using the well-known Langmuir–Hinshelwood and Cassie–Baxter models. k_p, k_c, and k_{-c} are the photocatalysis, adsorption, and desorption rate constants, respectively. f_s and f_{cs} are the area fractions of clean and oil-contaminated sites on the TiO_2 surface. $\theta^*_{w,o}$ is the water-in-oil contact angle of a sessile drop on the TiO_2 nanostructured surface.

When UV light illuminates a TiO_2 surface submerged in oil, three reactions can take place: adsorption and desorption of the hydrocarbon contaminant to the active sites plus photocatalytic destruction of the molecules adsorbed on the surface. Schematically, this can be described by the following process

$$S + C \underset{k_{-c}}{\overset{k_c}{\rightleftarrows}} SC \xrightarrow{k_p(h\nu)} S + P \tag{3}$$

where S and C represent the clean TiO_2 surface site and contaminant (hydrocarbon), respectively. SC represents the oil-adsorbed, that is, contaminated TiO_2 surface site and P, the product generated after photocatalysis. The rate constants for the adsorption, desorption, and photocatalytic destruction of oil are k_c, k_{-c}, and k_p, respectively. By assuming that the three reactions on the surface obey first-order kinetics,[45,50,51] we obtain a simple differential equation to describe the time-dependent area fraction of contaminated TiO_2 surface sites, $f_{sc}(t)$, given by

$$\frac{d}{dt} f_{sc}(t) = k_c f_s - k_{-c} f_{sc} - k_p f_{sc} \tag{4}$$

where f_s and f_{sc} are the area fractions of the neat and contaminated TiO_2 surface sites, respectively. Substituting $f_s = 1 - f_{sc}$ and solving Equation (4) results in

$$f_{sc}(t) = \frac{k_c}{k_c + k_{-c} + k_p} - \left(\frac{k_c}{k_c + k_{-c} + k_p} - f_{sc}(0) \right) e^{-(k_c + k_{-c} + k_p)t} \tag{5}$$

where $f_{sc}(0)$ is the initial area fraction of contaminated sites on the TiO_2 surface. Equation (5) suggests that a TiO_2 surface submerged in oil undergoes a time-dependent evolution in its surface chemical heterogeneity upon UV light illumination. A sessile droplet placed on a chemically heterogeneous surface will exhibit a contact angle given by the Cassie–Baxter equation (Equation (1)). If we assume that the under-oil contact angles for water on a completely uncontaminated nanotextured TiO_2 surface ($f_s = 1$) is $\theta^*_{w,o} = 0^\circ$ and that on a completely contaminated TiO_2 surface ($f_s = 0$) is $\theta^*_{w,o} = 180^\circ$, then the Cassie–Baxter equation is reduced to $\cos\theta^*_{w,o} = f_s \cos(0^\circ) + f_{sc} \cos(180^\circ) = 1 - 2f_{sc}$ (since $f_s + f_{sc} = 1$). By substituting f_{sc} in this expression with Equation (5), we finally obtain the following relationship describing the evolution in the measured effective contact angles for water on TiO_2 surfaces submerged in oil under UV light illumination

$$\cos\theta^*_{w,o}(t) = 1 - 2\left[\frac{k_c}{k_c + k_{-c} + k_p} - \left(\frac{k_c}{k_c + k_{-c} + k_p} - f_{sc}(0) \right) e^{-(k_c + k_{-c} + k_p)t} \right] \tag{6}$$

For convenience, we refer to this combined expression as "LuCY" (**L**angm**u**ir–Hinshelwood **C**assie–Baxter **Y**oung) model. In order to obtain the rate constants for adsorption (k_c) and desorption (k_{-c}) of oil on the nanotextured TiO_2 surfaces, we first apply the LuCY model to the data obtained during our contamination study. **Figure 5**a shows a plot of $\cos\theta^*_{w,o}$ as a function of contamination time. Note that we utilized the same values of $\theta^*_{w,o}$ that are shown in Figure 3a. Fitting our LuCY model to the experimental data gives the adsorption and desorption rate constants as $k_c = 3.54 \times 10^{-5} s^{-1}$ and $k_{-c} = 3.58 \times 10^{-7} s^{-1}$, respectively. Because the rate constant for surface adsorption (k_c) is two orders of magnitude higher than that for desorption (k_{-c}), it is evident that low-energy species such as hydrocarbon oils are readily adsorbed onto high-energy TiO_2 surfaces with increasing time.

Utilizing these values of the rate constants of adsorption and desorption, we estimated the rate constant for photocatalytic destruction (k_p) of adsorbed oil on TiO_2 surfaces using the data from experiments conducted under UV light illumination. Figure 5b shows a plot of $\cos\theta^*_{w,o}$ as a function of UV illumination time, constructed using the values of $\theta^*_{w,o}$ shown in Figure 3 b. The LuCY model was fitted to the experimental data to obtain the photocatalytic rate constants, $k_p = 7.1 \times 10^{-3} s^{-1}$, $k_p = 14.5 \times 10^{-3} s^{-1}$, and $k_p = 49.5 \times 10^{-3} s^{-1}$ for the intensities of $I = 40$, 120, and 200 mW cm^{-2}, respectively. The rate constants of photocatalysis (k_p) are several orders of magnitude higher than those of adsorption (k_c). This clearly indicates that the contaminated TiO_2 surface can be rapidly *cleaned* upon UV light illumination even under ongoing background contamination processes.

The values of k_p obtained using our LuCY model increase with increasing UV light intensity (see Figure 5b). This is because the rate of generation of charge carriers (i.e., electron–hole pairs) that degrade the organic species adsorbed on TiO_2 surfaces increases with increasing UV light intensity. However, as the concentration of electron–hole pairs rises, the rate of recombination becomes increasingly important under high-intensity UV light. The threshold intensity ($I_{threshold}$) at which this transition occurs lies in the range of 1–10 mW cm^{-2}.[47]

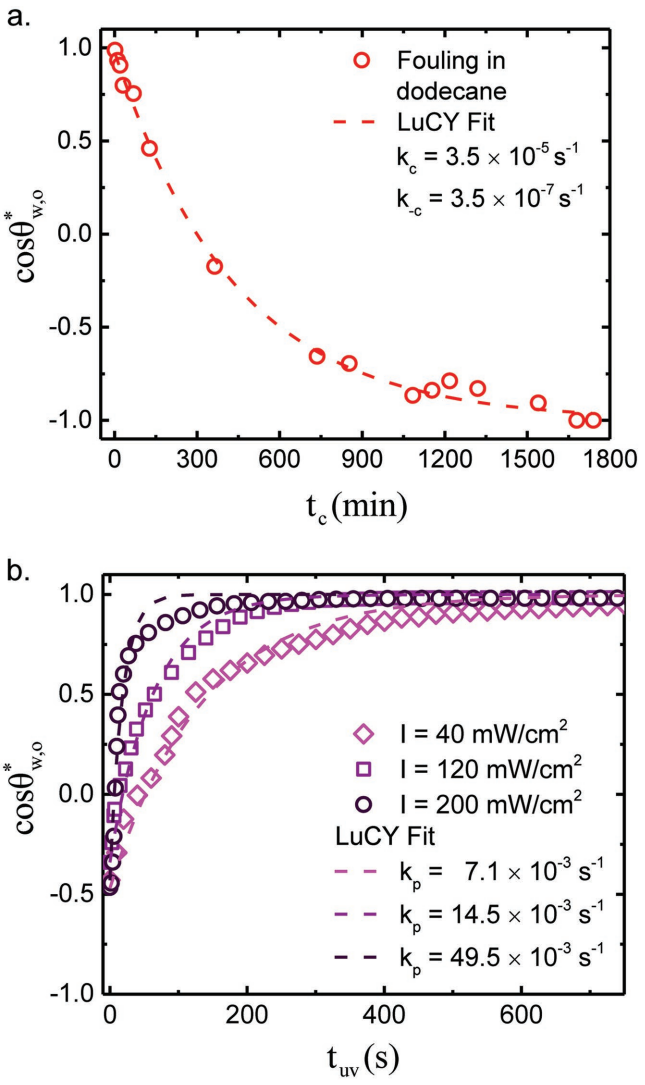

Figure 5. a) LuCY model fit and extraction of adsorption and desorption rate constants (k_c and k_{-c}, respectively) for an LBL-assembled nanostructured TiO_2 surface during contamination in dodecane; b) LuCY model fit and extraction of photocatalysis rate constants k_p for three intensities of UV irradiation on the same LBL TiO_2 surface.

Further, it has been reported that $k_p \propto I$ when $I < I_{threshold}$ whereas the rate constant increases more slowly as $k_p \propto \sqrt{I}$ when $I > I_{threshold}$. In **Figure 6**, we show a log-log plot of the measured rate constant for photocatalysis as a function of UV light intensity. We find that the k_p values obtained using our LuCY model are proportional to $I^{0.6\pm0.1}$ as expected for the UV light intensities we have investigated which are all higher than $I_{threshold}$.

Because our calibrated LuCY model provides a direct relation between the effective contact angles for sessile water droplets and the kinetics of surface reactions on the nanostructured TiO_2 surfaces under diverse conditions, it can also describe evolution in the size of a sessile droplet during illumination by UV which leads to photocatalytic cleaning of the surface. Assuming the volume of a droplet is conserved, the change in the contact angle is associated directly with changes in the base radius of the sessile droplet. From the hemispherical cap geometry shown in **Figure 7**a, the base radius (R_b) of a sessile droplet of water on the TiO_2 surfaces submerged in oil is given by[20]

$$R_b = \sin\theta^*_{w,o}\left(\frac{3}{\pi}\frac{V}{(1-\cos\theta^*_{w,o})^2(2+\cos\theta^*_{w,o})}\right)^{1/3} \quad (7)$$

where $\theta^*_{w,o}$, and V are the contact angle of the sessile drop of water immersed in oil, and the volume of a droplet, respectively. If two identical droplets of water (each with base radius R_b) are placed on a contaminated TiO_2 surface with distance $2d$ in between them (see Figure 7a) and then the surface is illuminated with UV light, we expect that the two droplets will coalesce when $R_b(t) = R_b(0) + d$. Figure 7b shows sequential images of the progressive coalescence of two droplets of water on the TiO_2 surface under UV light illumination (I = 400 mW cm^{-2}). Here, two droplets with identical base radius ($R_b(0)$ = 0.6 mm), volume (V = 3 µL), and initial under-oil contact angle ($\theta^*_{w,o}$ = 140°) are placed on the precontaminated TiO_2 surface (t_c = 18 h). The initial distance between the two droplets is $2d$ = 2.4 mm. Upon UV light illumination, the interfacial energy of the TiO_2 surface between the drops increases and the two droplets spread progressively over the surface and eventually coalesce. At this illumination intensity, we observe that coalescence occurs after a UV exposure time of t_{uv} = 80 s (denoted as $t_{coalesce}$ in Figure 7c). In Figure 7c, we show a plot of the measured and the predicted base radius R_b as a function of UV light illumination time. In order to predict the base radius, the value of the photocatalytic rate constant k_p(I = 400 mW cm^{-2}) was first evaluated using the power law fit in Figure 6. Then, this k_p value was used in Equation (6) to predict the evolution of the contact angles of the water droplets $\theta^*_{w,o}(t)$. Finally, the base radius $R_b(t)$ was calculated using $\theta^*_{w,o}(t)$ in Equation (7). Our LuCY model predicts that the drops will coalesce at time, $t_{predicted}$ = 68 s (see Figure 7c) which corresponds to $R_b = R_b(0) + d$ = 1.8 mm when the two droplets contact each other. Consequently, our LuCY model can be used to predict not only the evolution of the effective under-oil contact angles of water droplets but also the dynamic evolution in the base radius and coalescence of neighboring sessile drops on TiO_2 surfaces upon UV light illumination.

Since a droplet of water advances on the nanostructured TiO_2 surfaces under UV light illumination in an oil medium, an oil droplet placed on a TiO_2 surface in a water environment recedes from the surface in a similar way. Such photoinduced removal of oil from the surface has been exploited in fabricating self-cleaning surfaces.[33,36] Here, we demonstrate the self-cleaning of precontaminated TiO_2 surfaces on both nanoporous substrates and microtextured meshes submerged in water. **Figure 8**a shows sequential images of the self-cleaning process of TiO_2 surface fabricated on an impermeable (i.e., nonporous) glass slide. The surface is precontaminated by oil for 24 h and then submerged into water. Before photocatalyzed cleaning, the surface displays a low underwater oil contact angle $\theta^*_{o,w} = 30^\circ$. As the surface is illuminated by UV light (I = 240 mW cm^{-2}), photocatalysis increases the surface energy and hydrophilicity of the nanoporous LBL surface. We observe that the buoyant oil droplet recedes from the surface and beads up to form a sessile drop with a high contact angle. The droplet of oil can eventually be detached from the surface using a combination of external mechanical vibration

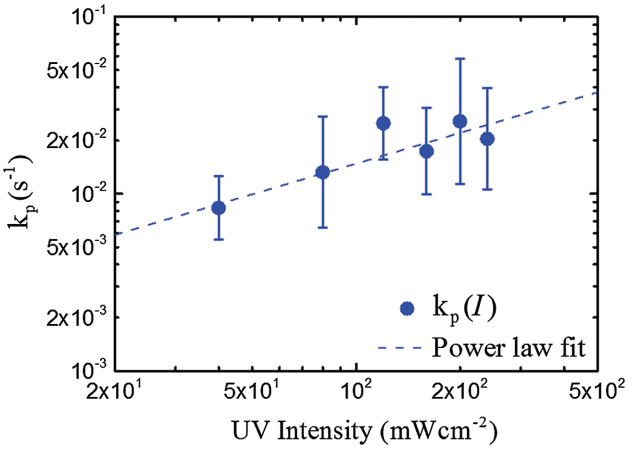

Figure 6. Dependence of photocatalysis rate constant k_p on UV intensity I. Linear regression to a functional form $k_p = \beta I^{\alpha}$ gives a power law coefficient of $\alpha = 0.6 \pm 0.1$.

(see Figure 8a) and the buoyant driving force ($\rho_o = 750$ kg m^{-3}). Figure 8b shows a plot of underwater oil contact angles ($\theta^*_{o,w}$) measured in situ on the TiO_2 surface submerged in water as a function of UV light illumination time. Note that we do not show the corresponding predictions of our theory in Figure 8b because the initial drop shape, radius, and volume of the oil droplet in this experiment could not be precisely controlled.[52]

We have also measured the self-cleaning capabilities of the nanoporous LBL-assembled TiO_2 coating on a microtextured substrate. In Figure 8c, we show sequential images of the beading up of an oil droplet from a contaminated (t_c = 24 h) stainless steel mesh (plain Dutch weave) that has been LBL-coated with 30 bilayers of TiO_2. During the contamination process, the oil permeates into the pores of the mesh and the hydrocarbon molecules adsorb onto the TiO_2 surface. After the onset of UV light illumination, the buoyant oil drop spontaneously recedes across the mesh surface and rearranges to form a single bead pinned to the upper surface of the mesh. Movie S2 (Supporting Information) shows self-cleaning of the mesh surface upon UV light illumination. The beaded up droplet separates from the mesh upon application of an external vibration because of the reduced wetted area of contact and thus the reduced interfacial adhesion between the textured mesh and the oil droplet. In oil–water membrane separations, the cross-flow of the feed water would perform the same task.[53]

3. Conclusion

We have studied the kinetics of wettability conversion of nanostructured TiO_2 surfaces under UV light illumination in an oil environment. We fabricated nanostructured surfaces for enhanced photocatalysis using LBL self-assembly of titania nanoparticles, and utilized in situ contact angle goniometry

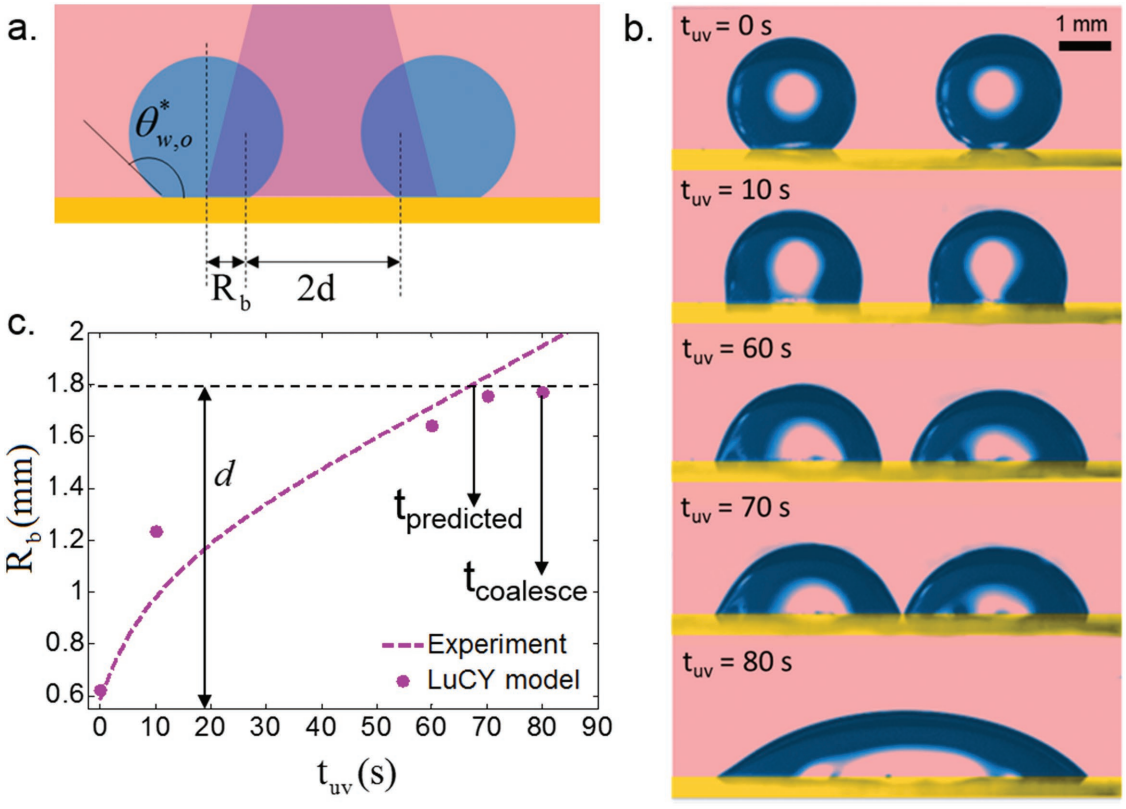

Figure 7. a) Schematic of a drop coalescence experiment showing the relevant geometric parameters and the section of the surface exposed to UV illumination (in violet shading); b) Coalescence of two identical drops of volume 3 µL under UV illumination (I = 400 mW cm^{-2}); c) Comparison of the evolution in drop base radius predicted by the LuCY model to the measured drop base radius.

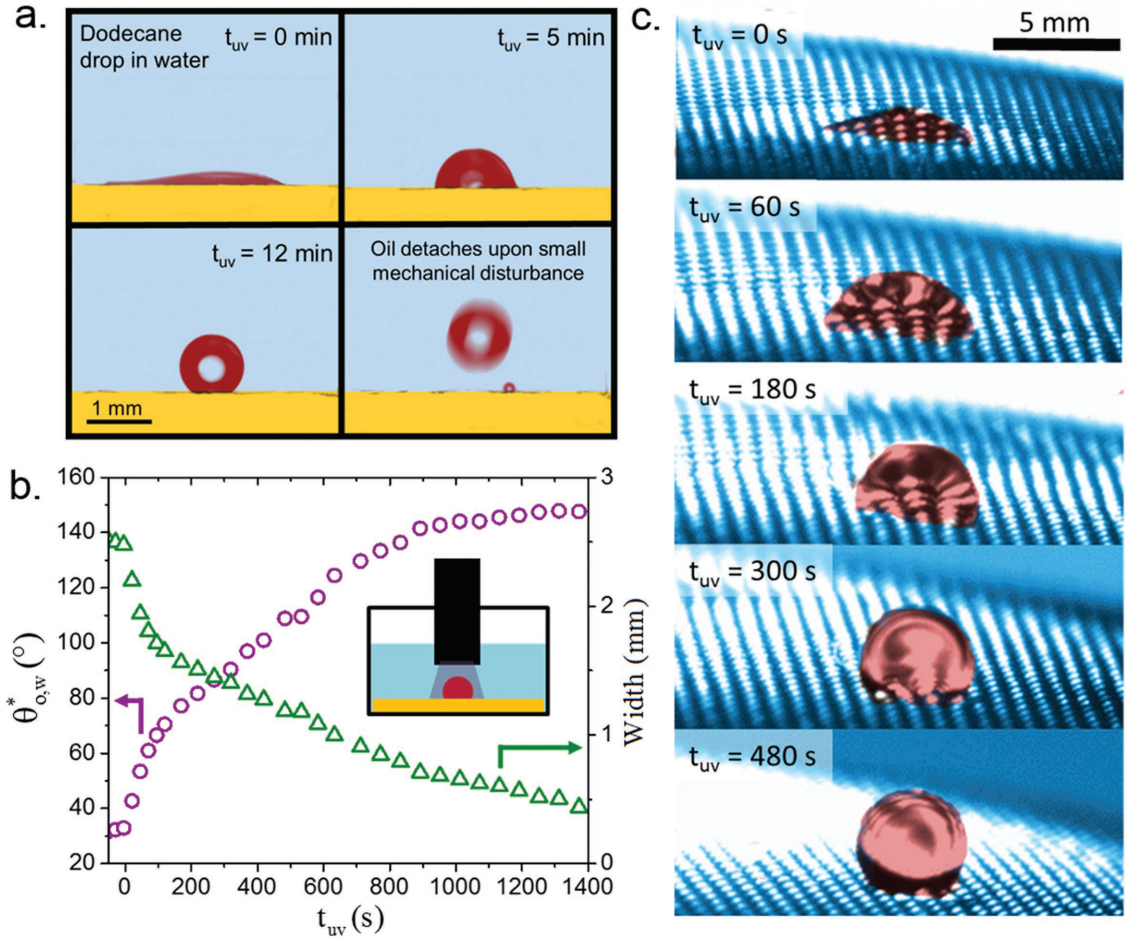

Figure 8. a) A sessile drop of oil beading up from the surface of an LBL nanostructured TiO_2 surface upon UV irradiation (I = 240 mW cm^{-2}); b) Evolution in the contact angle $\theta^*_{o,w}$ and width $2R_b(t)$ of oil drop versus time of irradiation (I = 240 mW cm^{-2}) on a flat glass surface; c) Drop of oil beading up from the pores of a precontaminated LBL TiO_2-coated stainless steel mesh (plain Dutch weave, wire diameter = 250 × 330 µm, wire spacing = 450 × 1100 µm) under water environment upon illumination of UV light (I = 300 W cm^{-2}).

to characterize the dynamics of surface reactions including the adsorption and desorption of hydrocarbons, as well as the photocatalytic decomposition of the adsorbed oil molecules on the TiO_2 surfaces. We propose a new kinetic model combining Langmuir–Hinshelwood kinetics and the Cassie–Baxter equation, which we refer to as "LuCY" that directly relates the UV-driven photocatalytic degradation of oil adsorbed on active sites of the catalyst to the evolution in the measured contact angles for sessile water drops submerged in an oil environment. Our LuCY model describes the evolution of the contact angles observed experimentally and also facilitates the extraction of the photocatalytic (k_p), adsorption (k_c), and desorption (k_{-c}) rate constants from goniometric data. We established from our experiments that k_p is much higher than both k_c and k_{-c}, implying that the rate of photocatalytic cleaning is much faster than the rate of hydrocarbon fouling for the range of UV intensities used. Measurements also show that $k_p \approx I^{0.6\pm0.1}$ for the range of UV intensities studied, in good agreement with existing photocatalysis literature. We have also demonstrated the applicability of this new kinetic model in canonical drop coalescence scenarios and membrane cleaning applications, and we envision that it may find applicability in designing and optimizing TiO_2-based surfaces for multiphase interfacial engineering applications such as oil–water separation.

4. Experimental Section

Materials: Glass slides (plain, VWR International), stainless steel mesh (TWP Inc., Plain Dutch Weave, image shown in Figure S1, Supporting Information), *n*-dodecane (anhydrous >99%, Sigma-Aldrich), aqueous dispersion of TiO_2 nanoparticles (Svaya Nanotechnology, average diameter ≈20 nm, 10% wt%), and poly(allylamine hydrochloride) (PAH, Sigma Aldrich, average molecular weight = 15 000 g mol^{-1}).

Layer-by-Layer Self-Assembly of TiO_2 Nanoparticles: The substrates were first sonicated in sodium hydroxide solution (10 wt%) for 1 h to remove any contaminants followed by thorough rinsing with DI water. They were then dried and treated with oxygen plasma on high power for 5 min in a basic plasma cleaner (PDC-001, Harrick Plasma). In order to perform LBL self-assembly of TiO_2 nanoparticles, a negatively charged TiO_2 dispersion, a positively charged polymer solution, and their respective rinse solutions were prepared in the following manner. Concentrated aqueous dispersion of TiO_2 nanoparticles (10 wt%) was diluted to 0.03 wt% in DI water. PAH was dissolved in water by stirring

for 2 h (concentration = 1 mg mL^{-1}). The pH of the PAH solution and TiO_2 dispersion were adjusted to 7.5 and 9.0, respectively, to give them positive and negative charges. Two aqueous solutions with pH 7.5 and pH 9.0 were also prepared using DI water, HCl, and NaOH, for rinsing substrates after dipping in the polymer and nanoparticle mixtures, respectively. The cleaned substrates were alternatingly spin-dipped (spinning speed 150 rpm) between the two aqueous mixtures for 10 min each using an automated multilayer dip-coating machine (StratoSequence 6, nanoStrata Inc.) to construct each bilayer. Two rinse steps of duration 2 and 1 min each were also performed between every layer to remove any excess deposits, and the substrates were dried in nitrogen gas for 30 s before the beginning of every layer. The substrates were removed and dried after deposition of 30 PAH/TiO_2 bilayers. They were then calcined at 400 °C for 2 h to remove the polymer from the assembled nanostructured film.

Characterization of Nanoporous Film: Scanning electron microscopy (FESEM Zeiss Ultra Plus), contact profilometry (Dektak 150), and ellipsometer (J.A. Woolham Co., VASE spectroscopic ellipsometer) were used.

Contact Angle Measurement: Goniometer (Ramé-Hart 590-F1) and quartz cell (Ramé-Hart P/N 100-07-50) were used.

UV Light Illumination: Spot UV light curing system (OmniCure S2000, Excelitas Technologies), liquid light guide (5 mm spot size, S series), visible light filter (Filter Band U-360 12 mm diameter, Edmund Optics), and UV radiometer (OmniCure UV Cure Site Radiometer R2000) were used.

Supporting Information

Supporting Information is available from the Wiley Online Library or from the author.

Acknowledgements

The authors would like to acknowledge financial support from King Fahd University of Petroleum and Minerals (KFUPM) through the Center for Clean Water and Clean Energy at MIT and KFUPM (Project No. R15-CW-11).

Conflict of Interest

The authors declare no conflict of interest.

Keywords

oil–water, photocatalysis, self-cleaning, titanium dioxide, wetting

Received: April 20, 2017
Revised: May 15, 2017
Published online:

[1] J. Drelich, E. Chibowski, D. D. Meng, K. Terpilowski, *Soft Matter* **2011**, *7*, 9804.
[2] X. J. Feng, L. Jiang, *Adv. Mater.* **2006**, *18*, 3063.
[3] J. Drelich, A. Marmur, *Surf. Innovations* **2014**, *2*, 211.
[4] K. Hashimoto, H. Irie, A. Fujishima, *Jpn. J. Appl. Phys.* **2005**, *44*, 8269.
[5] A. Fujishima, X. Zhang, D. A. Tryk, *Surf. Sci. Rep.* **2008**, *63*, 515.
[6] R. Wang, K. Hashimoto, A. Fujishima, M. Chikuni, E. Kojima, A. Kitamura, M. Shimohigoshi, T. Watanabe, *Nature* **1997**, *388*, 431.
[7] L. Zhang, R. Dillert, D. Bahnemann, M. Vormoor, *Energy Environ. Sci.* **2012**, *5*, 7491.
[8] S. Guldin, P. Kohn, M. Stefik, J. Song, G. Divitini, F. Ecarla, C. Ducati, U. Wiesner, U. Steiner, *Nano Lett.* **2013**, *13*, 5329.
[9] S. J. Gao, Z. Shi, W. B. Zhang, F. Zhang, J. Jin, *ACS Nano* **2014**, *8*, 6344.
[10] L. Li, Z. Liu, Q. Zhang, C. Meng, T. Zhang, J. Zhai, *J. Mater. Chem. A* **2015**, *3*, 1279.
[11] T. Zubkov, D. Stahl, T. L. Thompson, D. Panayotov, O. Diwald, J. T. Yates, *J. Phys. Chem. B* **2005**, *109*, 15454.
[12] J. M. White, J. Szanyi, M. A. Henderson, *J. Phys. Chem. B* **2003**, *107*, 9029.
[13] M. Takeuchi, K. Sakamoto, G. Martra, S. Coluccia, M. Anpo, *J. Phys. Chem. B* **2005**, *109*, 15422.
[14] C. Y. Wang, H. Groenzin, M. J. Shultz, *Langmuir* **2003**, *19*, 7330.
[15] K. Lee, Q. Kim, S. An, J. An, J. Kim, B. Kim, W. Jhe, *Proc. Natl. Acad. Sci. USA* **2014**, *111*, 5784.
[16] M. Miyauchi, N. Kieda, S. Hishita, T. Mitsuhashi, A. Nakajima, T. Watanabe, K. Hashimoto, *Surf. Sci.* **2002**, *511*, 401.
[17] M. Miyauchi, A. Nakajima, T. Watanabe, K. Hashimoto, *Chem. Mater.* **2002**, *14*, 2812.
[18] D. C. Hennessy, M. Pierce, K. C. Chang, S. Takakusagi, H. You, K. Uosaki, *Electrochim. Acta* **2008**, *53*, 6173.
[19] P. S. Foran, C. Boxall, K. R. Denison, *Langmuir* **2012**, *28*, 17647.
[20] K. Seki, M. Tachiya, *J. Phys. Chem. B* **2004**, *108*, 4806.
[21] M. Järn, Q. Xu, M. Lindén, *Langmuir* **2010**, *26*, 11330.
[22] E. B. Troughton, C. D. Bain, G. M. Whitesides, R. G. Nuzzo, D. L. Allara, M. D. Porter, *Langmuir* **1988**, *4*, 365.
[23] A. W. Adamson, *Physical Chemistry of Surfaces*, Wiley, New York **1982**.
[24] R. J. Good, L. A. Girifalco, *J. Phys. Chem.* **1960**, *64*, 561.
[25] A. J. Meuler, S. S. Chhatre, A. R. Nieves, J. M. Mabry, R. E. Cohen, G. H. McKinley, *Soft Matter* **2011**, *7*, 10122.
[26] S. Lee, Y. Aurelle, H. Roques, *J. Membr. Sci.* **1984**, *19*, 23.
[27] A. B. D. Cassie, S. Baxter, *Trans. Faraday Soc.* **1944**, *40*, 546.
[28] J. N. Israelachvili, M. L. Gee, *Langmuir* **1989**, *5*, 288.
[29] N. Sakai, A. Fujishima, T. Watanabe, K. Hashimoto, *J. Phys. Chem. B* **2003**, *107*, 1028.
[30] A. Nakajima, K. Hashimoto, T. Watanabe, K. Takai, G. Yamauchi, A. Fujishima, *Langmuir* **2000**, *16*, 7044.
[31] M. Textor, C. Sittig, V. Frauchiger, S. Tosatti, D. M. Brunette, *Titanium in Medicine*, Springer, Berlin, **2001**, pp. 171–230.
[32] Q. Chang, J. Zhou, Y. Wang, J. Liang, X. Zhang, S. Cerneaux, X. Wang, Z. Zhu, Y. Dong, *J. Membr. Sci.* **2014**, *456*, 128.
[33] A. Fujishima, T. N. Rao, D. A. Tryk, *J. Photochem. Photobiol., C* **2000**, *1*, 1.
[34] J. Yong, F. Chen, Q. Yang, U. Farooq, X. Hou, *J. Mater. Chem. A* **2015**, *3*, 10703.
[35] S. Nishimoto, Y. Mori, Y. Kameshima, M. Miyake, *Chem. Lett.* **2015**, *44*, 262.
[36] D. H. Kim, M. C. Jung, S. H. Cho, S. H. Kim, H. Y. Kim, H. J. Lee, K. H. Oh, M. W. Moon, *Sci. Rep.* **2015**, *5*, 12908.
[37] M. Liu, S. Wang, Z. Wei, Y. Song, L. Jiang, *Adv. Mater.* **2009**, *21*, 665.
[38] Y. C. Jung, B. Bhushan, *Langmuir* **2009**, *25*, 14165.
[39] A. Nakajima, S. I. Koizumi, T. Watanabe, K. Hashimoto, *Langmuir* **2000**, *16*, 7048.
[40] D. Lee, M. F. Rubner, R. E. Cohen, *Nano Lett.* **2006**, *6*, 2305.
[41] D. Lee, Z. Gemici, M. F. Rubner, R. E. Cohen, *Langmuir* **2007**, *23*, 8833.
[42] S. Nishimoto, Y. Sawai, Y. Kameshima, M. Miyake, *Chem. Lett.* **2014**, *43*, 518.
[43] S. Nishimoto, S. Tomoishi, Y. Kameshima, E. Fujii, M. Miyake, *J. Ceram. Soc. Jpn.* **2014**, *122*, 513.
[44] H. Y. Chen, O. Zahraa, M. Bouchy, *J. Photochem. Photobiol., A* **1997**, *108*, 37.

[45] S. M. Wetterer, D. J. Lavrich, T. Cummings, S. L. Bernasek, G. Scoles, *J. Phys. Chem. B* **1998**, *102*, 9266.
[46] A. Mills, J. Wang, D. F. Ollis, *J. Catal.* **2006**, *243*, 1.
[47] A. V. Emeline, V. Ryabchuk, N. Serpone, *J. Photochem. Photobiol., A* **2000**, *133*, 89.
[48] A. Mills, S. Le Hunte, *J. Photochem. Photobiol., A* **1997**, *108*, 1.
[49] A. Clark, *The Theory of Adsorption and Catalysis*, Academic, New York **1970**.
[50] E. Pelizzetti, C. Minero, V. Maurino, H. Hidaka, N. Serpone, R. Terzian, *Ann. Chim.* **1990**, *80*, 81.
[51] M. Sturini, F. Soana, A. Albini, *Tetrahedron* **2002**, *58*, 2943.
[52] Oil drop in water experiment: Here, the substrate was contaminated in oil for t_c = 18 h, as described in the paper and then removed and inserted into DI water. Once this surface is inserted into water, the oil film breaks up and beads up partially on parts of the substrate. UV light is subsequently irradiated upon one of these spots and the droplets recede as the photocatalytic process increases the surface energy and hydrophilicity of the surface. The initial drop shape, position, radius, and initial volume could not be precisely controlled in these experiments.
[53] B. Chakrabarty, A. K. Ghoshal, M. K. Purkait, *Chem. Eng. J.* **2010**, *165*, 447.

